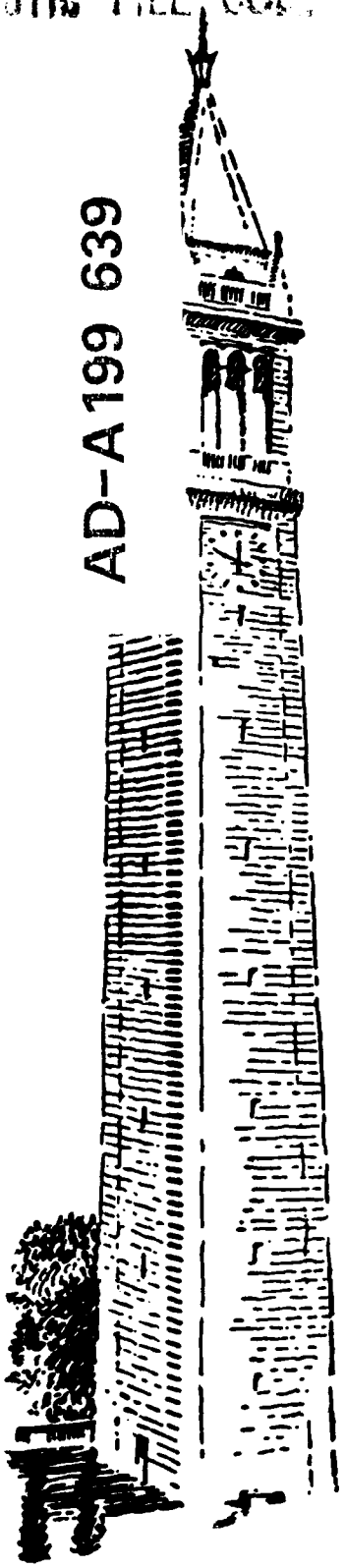

Contract N00014-85-K-0809

VORTEX FORMATION AND PARTICLE TRANSPORT IN A CROSS-FIELD PLASMA SHEATH

by

K. Theilhaber and C. K. Birdsall

Memorandum No. UCB/ERL-M88/53

10 August 1988

ELECTRONICS RESEARCH LABORATORY
College of Engineering
University of California, Berkeley, CA 94720

VORTEX FORMATION AND PARTICLE TRANSPORT IN A CROSS-FIELD PLASMA SHEATH

by

K. Theilhaber and C. K. Birdsall

Memorandum No. UCB/ERL M88/53

10 August 1988

ELECTRONICS RESEARCH LABORATORY

College of Engineering
University of California, Berkeley
94720

Vortex Formation and Particle Transport in a Cross-Field Plasma Sheath*

K. Theilhaber and C. K. Birdsall
Electronics Research Laboratory
University of California, Berkeley, CA 94720

Abstract

The time-dependent behavior of a transversely magnetized, two-dimensional plasma-wall sheath has been studied through particle simulations, which have shown that the cross-field sheath develops into a turbulent boundary layer, with strong potential fluctuations and anomalous particle transport. The driving mechanism is the Kelvin-Helmholtz instability, which arises from the sheared particle drifts created near the wall. The sheath acquires an equilibrium thickness $l_x \sim 5\ \rho_i$, and maintains large, long-lived vortices, with amplitudes $\delta\phi \sim -2T_i/e$, which drift parallel to the wall at roughly half the ion thermal velocity. The sheath also maintains a large, spatially-averaged potential drop from the wall to the plasma, in sharp distinction with the unmagnetized sheath, where the plasma potential is *higher* than at the wall. Accompanying the vortices is a spectrum of shorter-wavelength fluctuations which induce an anomalous cross-field transport. A central simulation result is that for $\omega_{pi} \geq 2\omega_{ci}$, the transport scales like Bohm diffusion, a result for which we have a qualitative analytic model.

*This is a shorter version of UCB/ERL M88/21, 20 March 1988 which has the same title. It has been submitted to *Physical Review Letters*.

Main Text

The following report on our particle simulations of the magnetized plasma-wall sheath. This is a study of plasma transport perpendicular to a magnetic field, in a plasma bounded by a conducting wall, with the aim of modelling the vicinity of the limiters and walls of magnetized plasma devices. Our approach has been to use our two-dimensional, bounded particle simulation code ES2 to investigate the edge effects which arise in such a configuration.

Our simulations have shown that the cross-field sheath between a wall and a plasma is not a static structure, but is in fact a turbulent boundary layer, with strong potential fluctuations and anomalous particle transport. The driving mechanism is the Kelvin-Helmholtz instability which arises from the sheared particle drifts created near the wall. Provided it is replenished by an internal flux of particles, the sheath will maintain itself in a dynamic equilibrium, in which the linear edge instability, the nonlinear plasma flows and the outward particle diffusion all balance each other. It is important to emphasize that the turbulent behavior of the sheath is a completely spontaneous phenomenon, which arises from the self-consistent plasma-wall interaction, and which does not require the imposition of external fields. This self-consistency, and the short space and time scales inherent in the plasma-wall interaction, sharply distinguish our work from previous simulations of the Kelvin-Helmholtz instability[1,2,3].

In Figs.(1), we show a series of snapshots of the electrostatic potential $\phi(x, y, t)$, in a system initially filled with a uniform distribution of electrons

and ions. Our simulation is two-dimensional and electrostatic[4], with the particles moving in the (x, y) plane, and subject to a magnetic field $\mathbf{B} = \hat{\mathbf{z}}B$. Periodic boundary conditions are imposed at the top and bottom of the simulation region ($y = 0$, L_y). The wall, at $x = 0$, is a perfect conductor and a perfect absorber of electrons and ions: when a particle hits the wall, its charge is immediately accounted for as mobile surface charge. The boundary conditions on the right-hand side, $x = L_x$, simulate a semi-infinite inner plasma: $x = L_x$ is an equipotential, and for the particles, an inversion symmetry condition is applied[5]. Finally, there is also a distributed plasma source, by which warm electron-ion pairs are created at a constant temporal rate, and with spatially random occurence. For Figs.(1), we have: $m_i/m_e = 40$, $T_i = T_e$, $\omega_{pi}/\omega_{ci} = 1.15$, $\omega_{pe}/\omega_{ce} = 0.18$, $\rho_i/\rho_e = 6.32$, and a system size $L_x/\rho_i = 5.06$ and $L_y/\rho_i = 40.5$. $N_e = N_i = 15000$ numerical particles of each species were initially in the system, with the creation rate (40 e-i pairs per ω_{ci}^{-1} time interval) adjusted to achieve similar steady-state values, $N_e \approx 16500$, $N_i \approx 14000$.

Fig.(1a), at $\omega_{ci}t = 15$, shows the essentially y-uniform sheath which has formed after just $2\frac{1}{2}$ rotations of the ions. This sheath is due to the initial loss of ions into the wall, resulting in a layer of depletion of positive charge in the plasma and a net positive charge on the wall. The result is a large potential drop from the wall into the plasma, $e\Delta\phi/T_i \approx -1.1$.

The sheath in Fig.(1a) contains a non-uniform electric field $E_x(x) > 0$, with maximum intensity at the wall, which induces a downward $\mathbf{E} \times \mathbf{B}$ drift of electrons and ions with a maximum velocity very close to the ion thermal speed, $v_y(x = 0) = -E_x(x = 0)/B \approx -v_{ti}$. Because the electric field is nonuniform, the resulting flow is strongly sheared, and is vulnerable to the

Kelvin-Helmholtz instability. In the subsequent evolution, noise grows into larger perturbations, which are both amplified and convected by the $\mathbf{E} \times \mathbf{B}$ flow. In Fig.(1b), the growing waves have amplitudes $e\delta\phi/T_i \approx -0.2$, and wavelength parallel to the wall $\lambda_y \approx 60$.

As the growing modes saturate, they form small vortices with approximate spacing $\lambda_y \approx 60$ (Fig.(1c)). These vortices, generated in $60 \leq \omega_{ci}t \sim 200$, are short-lived because they rapidly coalesce with each other, forming a smaller number of vortices with $\lambda_y \approx 120$. There is also simultaneous competition from the mode with $\lambda_y \approx 120$, which has a comparable linear growth rate. The overall effect is to favor the longer wavelength, and by $\omega_{ci}t = 250$, Fig.(1d), only two large vortices, each with $e\delta\phi/T_i \approx -1$ and $\lambda_y \approx 120$, have survived.

The two-vortex state of Fig.(1d) is only quasi-stable, because the vortices are once again vulnerable to the coalescence instability, and Figs.(1d,e,f) ($\omega_{ci}t = 250$, 375 and 437.5) show the progression to a single, large-amplitude vortex. This final vortex remains very stable throughout the remainder of the simulation, which we ended at $\omega_{ci}t = 1500$. It drifts parallel to the wall at a near-constant velocity $v_{0y} = -0.44v_{ti}$, and maintains $e\delta\phi/T_i \approx -2.2$. However, the background plasma remains fluctuating, and from time to time a smaller vortex is generated at some distance from the main vortex, eventually merging with the latter.

Overall, we have explored a range of parameters $0.5 \leq \omega_{pi}^2/\omega_{ci}^2 \leq 10$, with $\omega_{pe}^2/\omega_{ce}^2 \ll 1$, and have found behavior qualitatively very similar to the one outlined above. Simulations of broader systems than in Fig.(1) also show that the steady-state vortex and sheath acquire a "natural" thickness

of $l_x \approx 5\ \rho_i$, and do not grow indefinitely; thus the vortices are a feature of the sheath and not the bulk plasma.

To explain the evolution seen in Figs.(1), we have investigated the fluid cross-field equations. Assuming $|\omega| \ll \omega_{ci}$, we approximate the electron motion by the $\mathbf{E} \times \mathbf{B}$ drift, the ion motion by the $\mathbf{E} \times \mathbf{B}$ and polarization drifts[3], and obtain the coupled nonlinear equations:

$$\frac{m_i \epsilon_0 \omega_{ci}^2}{e^2} \frac{d}{dt} \nabla^2 \phi + \nabla \cdot \left(n \frac{d}{dt} \nabla \phi \right) = 0 \tag{1}$$

$$\frac{d}{dt} n = 0 \tag{2}$$

where $d/dt = \partial/\partial t + (\mathbf{E} \times \mathbf{B}/B) \cdot \nabla$ is the total derivative and $\nabla = (\partial_x, \partial_y)$. We then linearize Eqs.(1,2), in the presence of equilibrium profiles $v_0(x) = V_0 \hat{v}_0(x)$ and $n_0(x) = N_0 \hat{n}_0(x)$, with V_0 the velocity at the inflection point and N_0 the bulk plasma density, and $\hat{v}_0(x)$ and $\hat{n}_0(x)$ dimensionless profiles. With $\sigma \equiv \omega_{ci}^2/\omega_{pi}^2(n = N_0)$, we have the stability equation:

$$\frac{\partial^2}{\partial x^2} \phi_1 + \frac{\hat{n}_0'(x)}{\sigma + \hat{n}_0(x)} \frac{\partial}{\partial x} \phi_1 + \left(\frac{k_y}{\omega - k_y v_0(x)} \left(v_0''(x) + \frac{\hat{n}_0'(x) v_0'(x)}{\sigma + \hat{n}_0(x)} \right) - k_y^2 \right) \phi_1 = 0 \tag{3}$$

Taking $\hat{v}_0(x) = \tanh(x/a - 1) - 1$, and $\hat{n}_0(x) = \tanh(x/d)$, and fitting the parameters V_0, N_0, a and d to the conditions in the sheath at $\omega_{ci} t = 2\pi$, we find $V_0 = 0.51 v_{ti}$, $a = 0.63 \rho_i$, $d = 1.26 \rho_i$ and $\sigma = 0.73$. We then numerically solve Eq.(3) for $\omega = \omega_R + i\gamma$ as a function of k_y[2]. The results are shown in Fig.(2), where they are compared with the simulation results.

The predictions for the real part of the frequency agree reasonably well. On the other hand, while the growth-rates for the long-wavelength modes ($m = 1, 2$) are in agreement, fluid and simulation results diverge at the shorter wavelengths ($m = 3, 4, 5, 6$), an effect probably due to finite-larmor radius effects, but which we have not further investigated.

Turning to the nonlinear regime, we have attempted to model the final vortex by an approximate solution of Eqs.(1,2). We take the Navier-Stokes limit of Eqs.(1,2) (n = constant, or $\omega_{pi} \gg \omega_{ci}$), and then consider solutions which satisfy in a co-moving frame $\nabla^2\phi = f(\phi)$ [3,6]. Solutions with linear $f(\phi) = \alpha + \beta\phi$, as in[3,6], lead to vortices with amplitudes $e\delta|\phi|/T_i \ll 1$, in contradiction with simulation results. This suggests looking for more tightly-bound solutions, for instance with an exponential $f(\phi)$. In particular, the vortex chain of Stuart[3,7]:

$$\phi(x,y) = -v_0 x + \frac{v_0}{k_y}\log\left(\cosh(k_y(x-b)) + A\cos(k_y(y-v_0 t))\right) \qquad (4)$$

satisfies, in its rest-frame, the equation $\nabla^2\phi = k_y v_0 \exp(-2k_y\phi/v_0)$. With $k_y = 2\pi/L_y = 0.155/\rho_i$, $v_0 = -0.44 v_{ti}$, $b = 2.5\rho_i$ and $A = 0.57$, we have found that Eq.(4) gives a rough but sufficiently large-amplitude approximation to the observed vortex structure.

An essential feature of the cross-field sheath is the existence of a nearly constant, ambipolar transport of particles to the wall, for which we shall sketch a scenario: we believe that the ion motion, with a gyro-radius an appreciable fraction of the vortex dimensions ($\rho_i/l_x \approx 1/5$), is intrinsically stochastic, and readily leads to an outward ion diffusion, which is only

stopped by the positive charge building up at the wall. The electrons on the other hand are more strongly confined, and it is thus their rate of transport, induced by the edge turbulence, which determines the overall rate of transport for both species.

The orbits of test electrons show that their outward transport is the result of the $\mathbf{E} \times \mathbf{B}$ motion along broad orbits, trapped in or circulating about the vortices, combined with a shorter-scale diffusive motion, which we ascribe to the the high-frequency, short-wavelength fluctuations ($|\omega| \sim \omega_{ci}$, $|\mathbf{k}|\rho_i \sim 1$) which we see in the simulation power spectrum, and which accompany the vortices. Particularly vulnerable to scattering are the electrons on the vortex separatrix, their rapid loss leading to an evacuated region in front of the vortex. In the steady-state, we can define a time and space-averaged diffusion coefficient $D_x = sl_x^2/2\bar{n}(l_x)$, where l_x is the sheath thickness ($l_x = 5\rho_i$), s is the rate of pair creation (per unit area, per unit time), and $\bar{n}(l_x)$ is the y-averaged density in the plasma interior, assuming a parabolic $\bar{n}(x)$ in $0 \leq x \leq l_x$. The results for $\bar{D}_x$ from simulations with increasing creation rates, and hence increasing inner plasma densities, are shown in Fig.(3), where $\bar{\omega}_{pi}$ is evaluated at the spatially-averaged density. For $\bar{\omega}_{pi} \geq 2\omega_{ci}$, the diffusion coefficient has the Bohm-like dependence:

$$\bar{D}_x = 0.04 \frac{T_i}{eB} , \qquad \bar{\omega}_{pi} \geq 2\omega_{ci} \tag{5}$$

We have verified that the results in Fig.(3) are independent of plasma discreteness, by varying $\bar{n}\lambda_D^2$ in the range $4 \leq \bar{n}\lambda_D^2 \leq 56$, thereby confirming that transport is not collisional.

To provide a derivation of Eq.(5), we first assume that for $\omega_{pi} \gg \omega_{ci}$ the edge turbulence is density-independent. This is consistent with the $\omega_{pi} \gg \omega_{ci}$ limit of Eqs.(1,2). We then introduce "universal" parameters c_1, c_2 and c_3, with the vortex spacing $l_y = c_1\rho_i$, the vortex size $l_v = c_2\rho_i$, and the vortex depth $\phi_{max} = c_3 T_i/e$, with $c_1 \approx 40$, $c_2 \approx 5$ and $c_3 \approx 2$. Assuming a spectrum $< |\tilde{\phi}(k_y)|^2 >= A(k_y\rho_i) < |\tilde{\phi}(0)|^2 >$, and an wave-electron correlation time $\tau_c(k_y) = \omega_{ci}^{-1} T(k_y\rho_i)$, with the functions A and T independent of B, we then follow[8] and find an estimate which scales as in Eq.(5), $\bar{D}_z = c_0\ (T_i/eB)$, with constant c_0 given by: $c_0 = (1/\pi)(c_2c_3/c_1)^2 \int_0^\infty dK K^2 A(K)T(K)$. Assuming the integral to be of order 1, we find $c_0 = 0.02$, an estimate qualitatively in agreement with Eq.(5).

We have also studied the effects of finite $k_\parallel$, by tilting the magnetic field by a small angle $\theta = (m_e/m_i)^{1/2}/2$ from the perpendicular. With the field tilted *parallel* to the wall, the vortices are suppressed, and the edge turbulence and cross-field transport are greatly reduced, but the sheath maintains a large potential drop, $e\Delta\phi/T_i \approx -1.4$. With the field tilted *towards* the wall, the morphology is changed to that of the unmagnetized sheath, with electron flow dominant, and a potential *rise* from wall to plasma[9]. These results emphasize that the Kelvin-Helmholtz vortices arise for flute-like modes, forming only in regions of tangency to walls and limiters, or perhaps internally, across a separatrix.

Future simulations of the cross-field sheath should explore a larger range of parameters than possible in the present work. For instance, we believe that longer systems should accomodate many steady-state vortices. We were also limited to $\omega_{pi}^2/\omega_{ci}^2 \leq 10$ while we would like to explore values as

high as $\omega_{pi}^2/\omega_{ci}^2 = 10^3$, representative of a fusion environment. A straightforward modification of our simulation code, to allow for an $\mathbf{E} \times \mathbf{B}$ electron mover, should make these extended studies feasible at a reasonable cost in computer time.

The authors thank Dr.Liu Chen for many stimulating exchanges, and Dr.M.J.Gerver and Prof.A.J.Lichtenberg for various discussions. This research was supported by U.S. Department of Energy Contract No.FG03-86ER53220, by U.S. Office of Naval Research Contract No. N14-80-C-0507 and by a MICRO grant with a gift from the Varian Corporation.

References

[1] J.A. Byers, Phys. Fluids **9**, 1038 (1966).

[2] P.L. Pritchett and F.V. Coroniti, J. of Geo. Res., **89**, A1, 168 (1984).

[3] W. Horton, T. Tajima, T. Kamimura, Phys. Fluids **30**, 3485 (1987).

[4] C.K. Birdsall, A.B. Langdon, *Plasma Physics via Computer Simulation*, McGraw Hill, 1985, page 308.

[5] *Idem*, page 322.

[6] R.Z. Sagdeev, V.D. Shapiro, V.I. Shevchenko, Sov. Astron. Lett. **7**, 279, (1981).

[7] J.T. Stuart, J. Fluid Mech., **29**, part 3, 417 (1967).

[8] J.M. Dawson, H. Okuda, R.N. Carlile, Phys. Rev. Letters, **27**, 491 (1971).

[9] R. Chodura, Phys. Fluids **25**, 1628 (1982).

Figure Captions

Fig.(1): Contour plots of the electrostatic potential $\phi(x, y, t)$ taken during the particle simulation. The wall is at the left-hand boundary, $x = 0$.

Fig.(2): Comparison of fluid theory for the Kelvin-Helmholtz instability (full lines), with the simulation results (large dots); a) growth rates; b) real parts of the frequency. In Fig.(2b), v_0 is the vortex speed, $v_0 = 0.44 v_{th}$.

Fig.(3): Dependence of the time and space-averaged diffusion coefficient on the steady-state density.

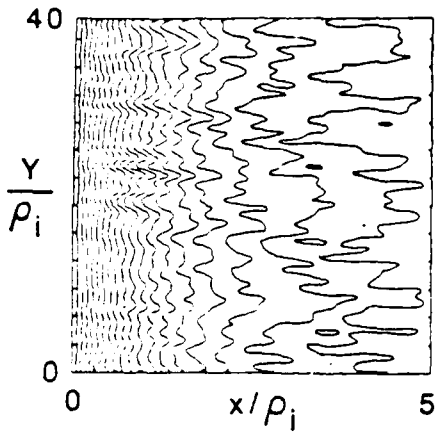

a) $\omega_{ci}t$=15

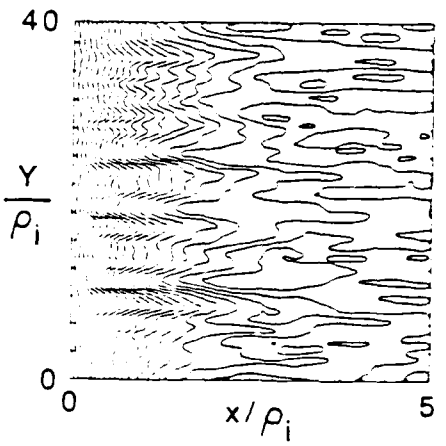

b) $\omega_{ci}t$=62.5

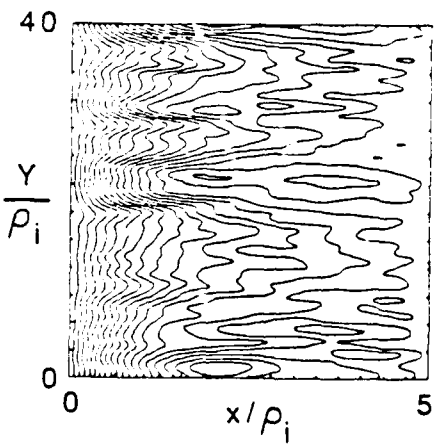

c) $\omega_{ci}t$=125

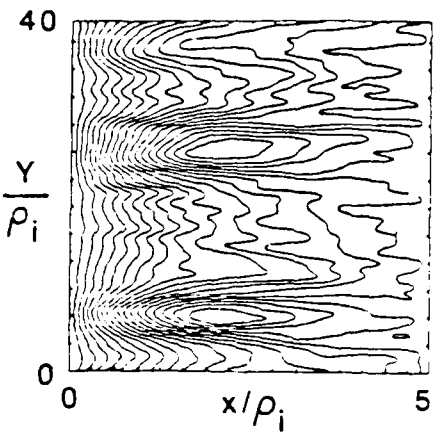

d) $\omega_{ci}t$=250

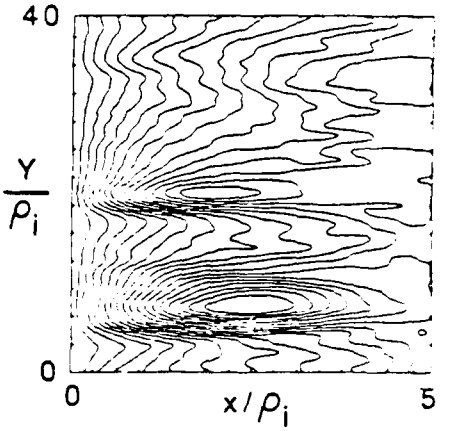

e) $\omega_{ci}t$=375

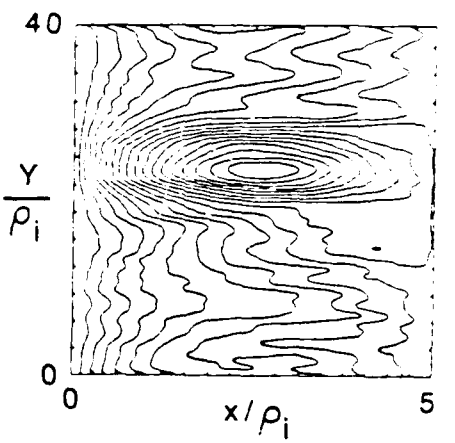

f) $\omega_{ci}t$=437.5

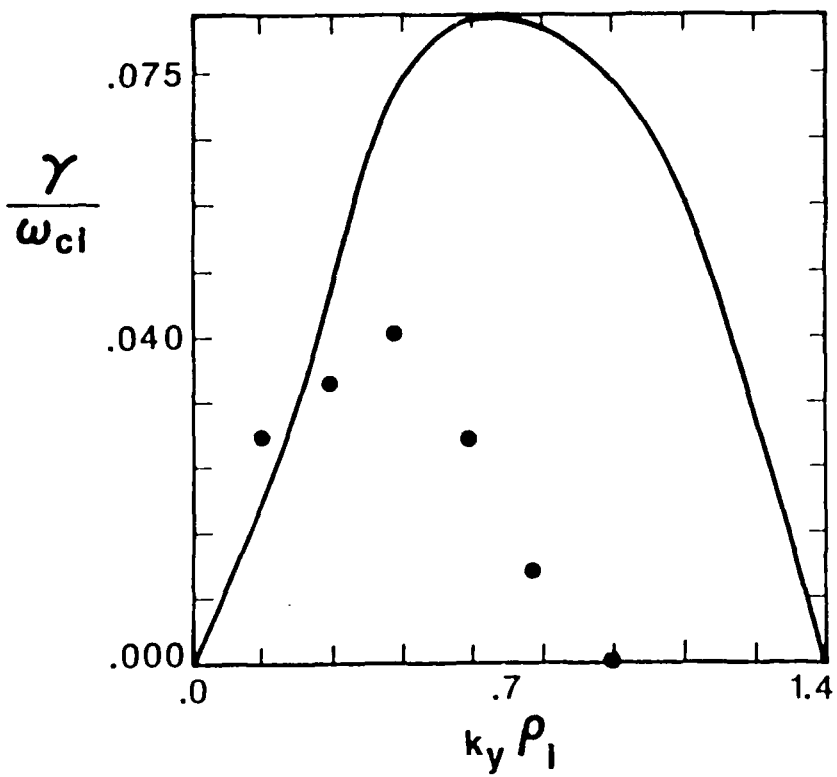
$\frac{\gamma}{\omega_{ci}}$
.075
.040
.000
.0
.7
1.4
$k_y \rho_i$

(a)

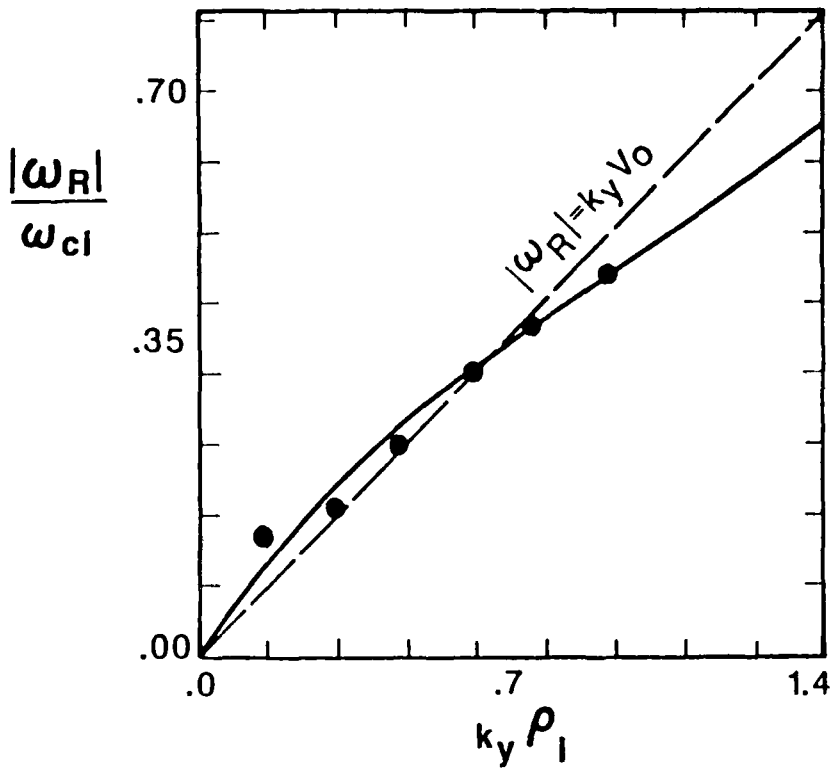
$\frac{|\omega_R|}{\omega_{ci}}$
.70
.35
.00
.0
.7
1.4
$k_y \rho_i$
$|\omega_R| = k_y V_o$

(b)

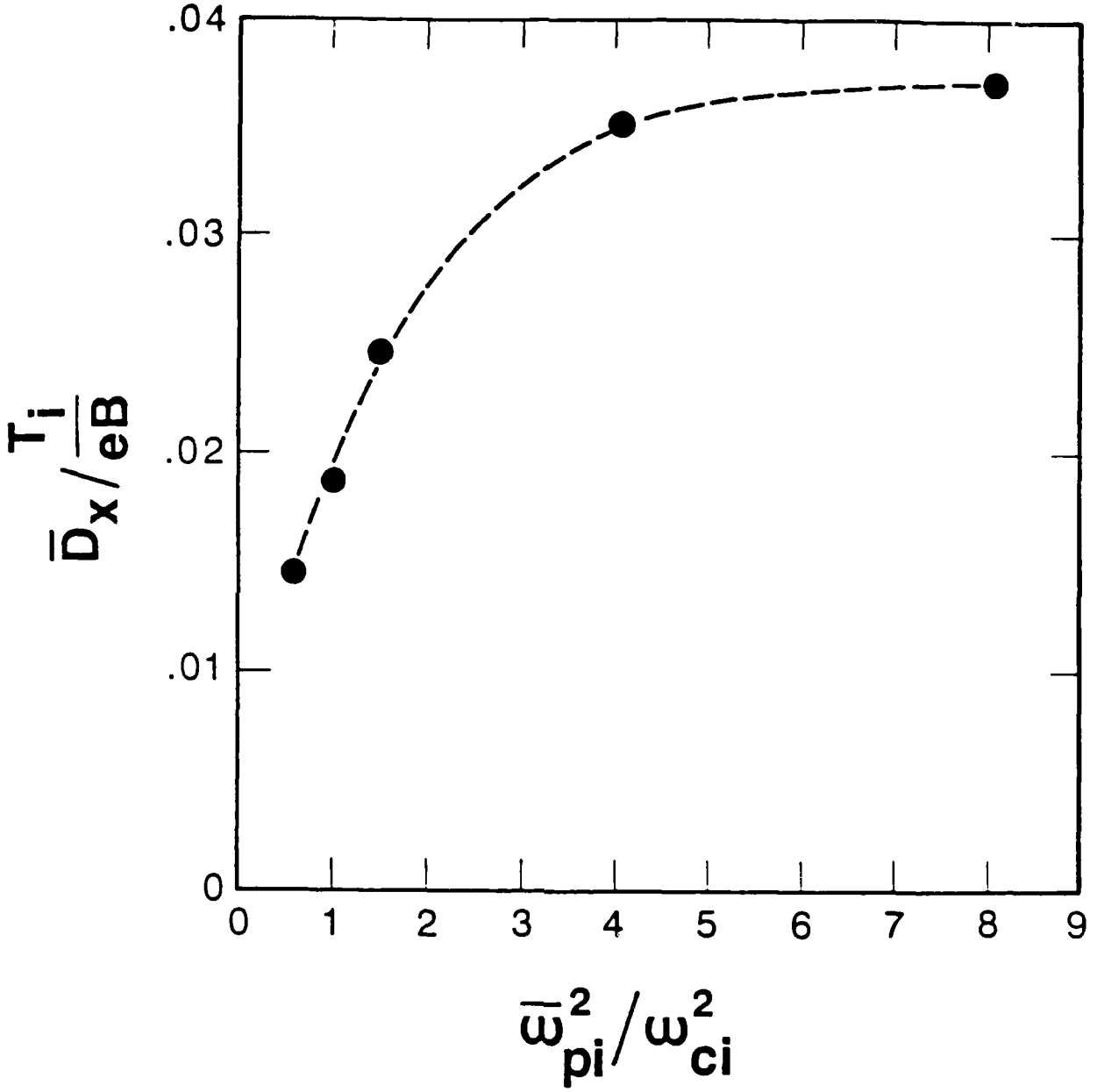
.04
.03
.02
.01
0
0
1
2
3
4
5
6
7
8
9
$\frac{T_i}{\bar{D}_x/eB}$
$\bar{\omega}_{pi}^2/\omega_{ci}^2$